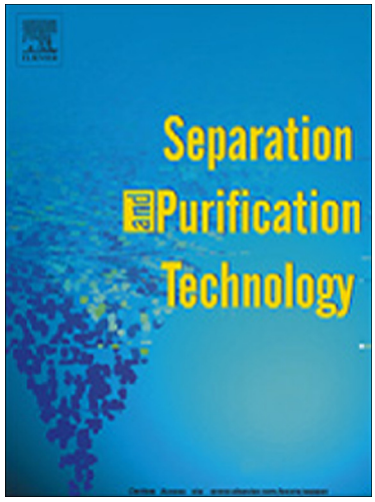

Image Analysis of Sludge Aggregates

Lech Smoczyński, Harsha Ratnaweera, Marta Kosobucka, Michał Smoczyński

PII: S1383-5866(13)00567-4
DOI: http://dx.doi.org/10.1016/j.seppur.2013.09.030
Reference: SEPPUR 11415

To appear in: *Separation and Purification Technology*

Received Date: 8 July 2013
Revised Date: 24 September 2013
Accepted Date: 28 September 2013

Please cite this article as: L. Smoczyński, H. Ratnaweera, M. Kosobucka, M. Smoczyński, Image Analysis of Sludge Aggregates, *Separation and Purification Technology* (2013), doi: http://dx.doi.org/10.1016/j.seppur.2013.09.030

Image Analysis of Sludge Aggregates

Lech Smoczyński [a*], Harsha Ratnaweera [b], Marta Kosobucka [a], Michał Smoczyński [c]

[a] Department of Chemistry, Faculty of Environmental Management and Agriculture, University of Warmia and Mazury in Olsztyn, Poland
[b] Department of Mathematical Sciences and Technology, Norwegian University of Life Sciences, Aas, Norway
[c] Department of Dairy Science and Quality Management, Faculty of Food Sciences, University of Warmia and Mazury in Olsztyn, Poland

[*] Corresponding author: Department of Chemistry, Faculty of Environmental Management and Agriculture, University of Warmia and Mazury in Olsztyn, Poland. Tel.: +48 89 5233668; fax: +48 89 5234801. E-mail address: lechs@uwm.edu.pl (L. Smoczyński).

A B S T R A C T

This study investigates the hypothesis that the mechanisms of chemical coagulation-flocculation and electrocoagulation produce specific imprints in nature, and the structure of sludge aggregates-floccules (flocs). Scanning electron microscopy (SEM) methods were used to produce 480 images of 32 types of wastewater sludge. The analyzed sludge was obtained by chemical coagulation and electrocoagulation of four types of synthetic effluents containing four red dyes. Perimeter P and area A of 120-170 differently sized objects were determined in 256 selected and contrast-enhanced images with the use of Image Analysis software. $lgA \sim lgP$ plots revealed that the analyzed sludge samples were made of self-similar aggregates-flocs with fractal characteristics. The slope s of log plots was used to determine surface fractal dimension D_a which was extrapolated to volumetric fractal dimension D_v. Dimension D_v was applied in a quantitative description of sludge aggregates-flocs. Aggregates-flocs of Al sludge group were characterized by higher values of D_v in comparison with Fe sludge group, which quantitatively confirmed the compactness of Al sludges and the jagged character of Fe sludges observed in SEM analyses. No flocculation of dye alone was observed, but the results of the experiment showed that phosphates were required for the destabilization of the colloidal system containing dye. In view of the above, a simple model of P-PO_4 and dye sorption on a colloidal sorbent made of {$Al(OH)_3$} or {$Fe(OH)_3$} was proposed. The structure of {$Al(OH)_3$} and {$Fe(OH)_3$} aggregate-flocs was graphically simulated to determine the effect of volumetric fractal dimension D_v on sweep flocculation and sludge separation and dehydration. The modeled processes of P-PO_4 sorption and sweep flocculation of dyes and the simulated images of aggregate-flocs confirmed that the analyzed wastewater sludges were mainly formed in the process of diffusion limited cluster-cluster aggregation DLCA, even the particle-cluster type aggregation with pre-polymerized coagulants (PAC) could be involved.

Keywords: sludge separation, SEM image analysis, floc simulation.

1. Introduction

Irreversible aggregation [1] produces larger assemblages which are referred to as sludge agglomerates, aggregates, clusters or flocs. Aggregation has important physiological and immunological implications [2]. The process is observed in nature, it is used in food technology and in the production of polymers. The main stages of aggregation, such as those observed during the destabilization of colloidal particles in wastewater, are processes of latent coagulation and active heterocoagulation [3] that lead to flocculation [4, 5], i.e. the formation of aggregates-flocs [6]. Clusters formed during wastewater flocculation are referred to as sludge flocs. The separation of sludge flocs by sedimentation or floating [7] removes various pollutants from the liquid phase of treated effluents. Sludge separation is a fundamental process in the recovery and recirculation of wastewater nutrients, including phosphorus, and it can effectively counteract the growing deficit in this fertilizer component [8].

Image analysis becomes a common methodology in many research areas [9]. Chemical coagulation-flocculation [4, 10-11] and electrocoagulation [12-14] leave imprints in nature and the structure of sludge aggregates-flocs. Those imprints can be visible also in their images. "Self-similarity" [15], i.e. the similarity of observed structures regardless of the applied scale of magnification (or reduction), is generally indicative of their fractal character [16]. Statistically documented self-similarity of a given group of sludge flocs usually supports determinations of their fractal dimension D [17-19]. The value of D can define the degree to which space is filled with matter and, consequently, the spatial structure of a sludge aggregate-floc. Jagged shape and large surface area should contribute to aggregates-flocs' sorption capacity during sweep flocculation [4]. Dense aggregates-flocs should generate sludge which is easily separated from the treated effluent phase. Dense sludge should be susceptible to dehydration in an ultracentrifuge or a filter press.

Variations in D values of the investigated structures could also be indicative of similarities and differences in coagulation-aggregation-flocculation mechanisms responsible for the formation of manageable sludge [18-22]. Two main models of the aggregation process have been proposed: a) particle-cluster aggregation (PA) and b) cluster-cluster aggregation (CA). Indirect mechanisms can also be involved, such as PA in initial stages of aggregation which is transformed to CA in final stages of the process. Computer models of cluster formation [3, 21] suggest that aggregates formed during PA are larger than those created during CA. The results of laboratory research investigating natural systems [23], such as

municipal sewage, indicate that fractal dimensions of aggregates are determined by coagulant concentrations [24]. Computer simulations have demonstrated that the fractal dimension of aggregates produced/simulated by CA can vary significantly with regard to aggregation speed. Asnaghi [25] identified two types of aggregation processes: a) diffusion-limited cluster aggregation (DLCA), b) reaction-limited cluster aggregation (RLCA), whereas c) ballistic cluster aggregation (BCA) is also taken into account in theoretical calculations [26]. In most cases, aggregates formed by RLCA have higher fractal dimension *D* than flocs produced by DLCA.

In this study, we have compared and interpreted the values of fractal dimension *D* determined from SEM images of sludges produced through chemical coagulation and electrocoagulation of synthetic wastewater. Though the proposed method for analyzing wastewater sludge is probably not a comprehensive method, it supplements the existing methods contibuting new and valuable information. It illustrates certain trends which require further investigation, development and improvement.

2. Materials and methods

The presence of red dyes in treated wastewater is highly undesirable. The investigated aqueous solutions of Direct Red 6B, Synten Red P-3BL, Gryfalan Red G and Synten Orange P-4RL were not susceptible to chemical coagulation or electrocoagulation, but mixtures combining the above dyes with phosphate ions, in particular milk powder, were highly sensitive to coagulation and electrocoagulation. The analyzed group of 32 sludges was broken down into four main categories of synthetic effluents under nearly optimal treatment conditions:

a) DDS – chemically coagulated discharges from dairy plants, dye plants and municipal wastewater treatment plants,
b) DSch – chemically coagulated discharges from dye plants and municipal wastewater treatment plants,
c) DSes – statically electrocoagulated discharges from dye plants and municipal wastewater treatment plants,
d) DSre – recirculated and electrocoagulated discharges from dye plants and municipal wastewater treatment plants.

1 dm^3 of DSch, DSes and DSre effluents contained 11-13 drops of saturated NaCl solution (to increase specific conductance κ to 0.4 S/m), 100 ml of the respective dye and 100 mg of $P\text{-}PO_4$. 1 dm^3 of DDS discharges was additionally mixed with 10 g of Nestle milk

powder to produce initial COD_o of 15500 ± 200 $mg \cdot dm^{-3}$ (average from 23 replications). Subject to need, the pH of treated wastewater was adjusted with 1M of NaOH or HCl solution. 1 dm^3 of DDS and DSch was chemically coagulated with 139 mg of Al-based PAC coagulant (Flokor 1A [www.dempol.com.pl]) or 171 mg of Fe-based PIX coagulant (PIX113 [www.kemipol.com.pl]). DDS coagulation was additionally enhanced with Silica Ludox [www.sigmaaldrich.com]. Chronopotentiometric electrocoagulation [14] of DSes (optimal time of 256-1024 seconds) and DSre effluents (3840 seconds) was carried out with the use of aluminum or iron electrodes at I = 0.3 A [13]. The applied coagulant and electrocoagulant doses guaranteed controlled and nearly complete transfer of $P\text{-}PO_4$ and dye from the treated wastewater solution to sludge separated by sedimentation. Coagulation removed >90% of $P\text{-}PO_4$ and dye from DDS, and sludge contained approximately 55% of organic substances responsible for COD. Coagulation and electrocoagulation (chronopotentiometric) procedures are described in detail in the Results and Discussion section.

Sludges were dried at the temperature of 105°C on mesh screens. The 1-2 mm fraction was separated from 32 sludge samples (16 Al sludges and 16 Fe sludges) and examined under the Quanta FEG 250 scanning electron microscope [www.biotech.iastate.edu/publications/news_releases/images/quanta.pdf]. Images from five sample locations were registered in accordance with the diagram presented in Figure 1.

Fig. 1

The above procedure was repeated three times to produce 15 images of every sludge sample, of which eight images with a similar structural pattern were selected. Each of the eight images was processed using the Image Analysis program (NIS-Elements Basic Research on Nikon [www.nis-elements.com/br.html]) to produce images with constant maximum contrast of *high –106, low – 105*. The perimeter (*P*) and area (*A*) of 120-170 small, medium and large objects were measured. $lg\ A \sim lg\ P$ plots were characterized by coefficient of determination R^2 in the range of 0.937 to 0.976 with average $R^2 = 0.963$ (Table 3). The analyzed objects were self-similar and their "surface" fractal dimension D_a was calculated from the slope of the respective $lg\ A = f(lg\ P)$ line [18, 27]. Two highest and two smallest values were rejected in every set of eight values of D_a, and average D_a was calculated from the remaining four values. Standard deviation was determined from the value of D_v after the conversion of D_a do D_v. The procedure is described in detail in the Results and Discussion section.

3. Results and discussion

Static electrocoagulation was performed chronopotentiometrically at I_{const} = 0.3A for 256 to 1024 s with the use of a simple device presented in Figure 2.

Fig. 2.

To determine the actual doses of Al and Fe, 100x10x1 mm electrodes were weighed before and after use in accordance with the rinsing and drying procedure described in a previous study [28].

Electrocoagulation in a recirculation system was also performed chronopotentiometrically at I_{const} = 0.3A for 3840 s with the use of a device presented in Figure 3.

Fig. 3.

1 dm^3 of DSre wastewater with composition identical to DSes was recirculated between reservoir *C* and electrolyzer *E* for 3840 s.

Table 1.

Treatment parameters of the analyzed effluents are presented in Table 1. DDS and DSch wastewater was chemically coagulated with the use of fixed coagulant doses at 5 drops per 200 cm^3 of effluent, i.e. 139 mg of Al-based PAC coagulant and 171 mg of Fe-based PIX coagulant. DDS wastewater was coagulated at the optimal pH of 5. The coagulation process was enhanced with optimal doses of Silica Ludox at 0.20-0.40 mg SiO_2/dm^3 wastewater for the PAC coagulant and 0.20-0.40 mg SiO_2/dm^3 wastewater for the PIX coagulant. Silicon dioxide increased COD removal by 15%, dye removal by 68% and $P\text{-}PO_4$ removal by 58% (Table 2). The above procedure produced eight types of sludge: four sludges for four dyes with PAC and four sludges for four dyes with PIX.

DSch and DSes effluents were coagulated at optimal pH of 3.5 to 4.5. Owing to the simplicity of the laboratory device and the applied electrocoagulant doses, DSes wastewater could be estimated gravimetrically during static electrocoagulation. Electrodes were weighed before and after electrocoagulation in accordance with the rinsing and drying procedure described in [28]. Sludges produced by high doses of the Al electrocoagulant should be rich in

{$Al(OH)_3$}. Electrocoagulant doses applied during electrocoagulation of DSre effluents in a recirculation system were determined based on Faraday's law:

$$m = k \cdot I \cdot t \qquad \text{where:} \quad k_{Al} = 9\ g \cdot F^{-1} \ \text{and} \ k_{Al} = 28\ g \cdot F^{-1}$$

on the assumption that anodic dissolution of aluminum and iron is characterized by 100% efficiency. The Fe ion dose was determined at 333 mg/dm^3 wastewater, and the Al ion dose at 107 mg/dm^3 wastewater. In view of previous research results [28], the actual Al ion dose was probably higher. The optimal pH of DSre effluents treated with Al electrodes was 6.0 and with Fe electrodes – 4.0.

Table 2.

The percentage of P-PO_4 and dye removed and separated from treated wastewater during sedimentation is presented in Table 2. The addition of silicon dioxide supported >90% removal of P-PO_4 and dye from treated DDS effluent, including gryfalan dyes which are weakly susceptible to the coagulation of DSch, DSes and DSre effluents. PAC was less effective than PIX in removing P-PO_4 from DSch wastewater. Electrocoagulation in a recirculation system (DSre) was more effective when Al rather than Fe electrodes were applied. In general, similar quantities of P-PO_4 and dye were removed from treated effluents.

The SEM analysis produced 480 sludge images, including 240 with the use of an aluminum coagulant or electrocoagulant in Al sludges and 240 with the use of an iron coagulant or electrocoagulant in Fe sludges.

Fig. 4.

Nine out of 480 images of sludge produced by chemical coagulation (*a, b*) and electrocoagulation (*c, d*) are presented in Figure 9. Similar SEM images of wastewater sludge were described by Verma [29]. The top four Al images correspond to sludges produced by chemical coagulation with PAC or by electrocoagulation with Al electrodes. The bottom four Fe images illustrate sludges produced by chemical coagulation with PIX or by electrocoagulation with Fe electrodes. Although four electrocoagulated sludges (*c, d*) were obtained with the use of different electrocoagulants (Al and Fe) and under different electrocoagulation conditions (*c* – static, *d* – recirculation), no significant differences were observed in their structure. The structure of four *a* and *b* sludges differs from that of four *c*

and *d* sludges which were produced in different processes of chemical coagulation (*a, b*) and electrocoagulation (*c, d*). The sludges obtained from DSch effluents (*b*) were characterized by a more homogenous structure than DDS sludges (*a*), which can be attributed to a less varied composition of DDS than DSch effluents. DDS wastewater was represented by "DSch + SiO_2 + milk", therefore, similarly to DSch effluents, the resulting sludge contained $\{(OH)_n(Al)_m(PO_4)_x(dyestuff)_y\}$ flocs as well as other chemical bonds with SiO_2 and milk powder ingredients. The most significant structural variations were reported between sludges obtained with PAC (*a, b* – top) and PIX (*a, b* – bottom). Structural objects in DDS sludges produced with PIX (*a* – bottom) were small, needle-shaped and jagged, whereas the objects forming the structure of sludges produced with PAC (*a* – top) were round and compact. The noted differences can be attributed to the spherical shape of $\{Al(OH)_3\}$ colloidal particles and the rod-like and cylindrical shape of $\{Fe(OH)_3\}$ particles [30-31]. Those particles are the building blocks of clusters which aggregate and flocculate to produce sludge flocs. The remaining four electrocoagulated sludges were characterized by minor structural differences. The observed variations were quantitatively confirmed in successive parts of this study.

A visual inspection of 480 images revealed that the applied dye did not exert a clear and unambiguous effect on sludge structure. The only exception was the group of sludges formed by static electrocoagulation of DSes effluents containing Synten Orange P-4RL with Fe electrodes. For this reason, an additional, ninth image of the above sludge was presented in Figure 4 in group *c*. In the analyzed group of dyes, Synten Orange P-4RL was characterized by the smallest particles with relatively linear structure, which could have contributed to the formation of cylinder/rod/wire-shaped aggregates-flocs whose structure was characteristic of $\{Fe(OH)_3\}$ colloidal particles described by Haas [30] and Rohrserzer [31]. Distinctive $\{Fe(OH)_3\}$ structures were not observed in DSes-Fe effluents containing other dyes or DSre-Fe effluents containing Synten Orange P-4RL.

Descriptions of SEM images can be further elaborated, but this approach does not produce constructive or fundamental conclusions. The number of sludges was initially reduced to 256 (eight images were selected from a group of 15 – refer to the previous section) for a quantitative description of structural objects in the analyzed sludges. The images of 256 sludges were displayed in maximum black and white contrast in the Image Analysis application with the following contrast settings: *high - 106, low - 105.* The above procedure emphasized certain characteristic shapes, traits and differences.

Fig. 5.

The images shown in Figure 4 were enhanced with maximum contrast and presented in Figure 5. The resulting images resemble maps with clear contours of shapes identifiable in SEM images. In contrast with cylinder- and rod-shaped structure of Fe aggregates, the spherical nature of Al aggregates supports the identification of certain structural "symptoms" under maximum contrast. The presence of jagged and uneven structures is difficult to quantify with a naked eye, and qualitative and quantitative comparisons supporting the classification of the analyzed images into groups are impossible to perform. The NIS-Elements Basic Research software (Nikon, Japan) facilitates observations and comparison of complex structures.

The above software was used in the successive stage of the study to analyze the structure of each of 256 contrasted images. Random white objects, classified as a) very large, b) large, c) medium-sized, d) small and e) very small, were selected manually. By clicking on a given white image, similar objects were automatically indicated in the analyzed image. The selection of a white object eliminated all disturbances caused by black surface cracks which were observed in selected images. A total of 120 to 170 white spots were identified in each of the 256 images. The predominant size of the analyzed objects and the subjective contrast of images shown in Figure 4 did not affect self-similarity. The Image Analysis application measured area A and perimeter P of all objects, including manually and automatically (majority) selected objects. The resulting data were used to develop $lg\ A \sim lg\ P$ plots and charts illustrating the distribution of object dimensions.

Fig. 6.

Sample $lg\ A \sim lg\ P$ plots of images shown in Figures 4d and 5d (DSre-Al and DSre-Fe) are presented in Figure 6. They are accompanied by charts illustrating the distribution of R values (in μm) of surface objects to determine fractal dimension D_v. The database in Figure 6 is described in detail in successive parts of this paper. It was used in calculations, simulations and models of sludge aggregates-flocs obtained by electrocoagulation of DSre effluents in a recirculation system.

A total of 256 plots and 256 distribution charts were produced for 32 sludge types in eight replications, and the respective average values are shown in Table 3. The analysis focused on objects characterized by significant variations in diameter from approximately 10 μm to approximately 100 μm. The range of variations in objects selected from the surface of the examined images is sufficient to ascertain the self-similarity of the analyzed objects. The

parameter which validates the significant self-similarity of the identified objects is the high value of coefficient of determination R^2 which was calculated separately for every $lg\ A \sim lg\ P$ plot. In all 256 plots, R^2 always exceeded 0.915. This implies that the applied mathematical model of $lg\ A = f(lg\ P)$ adequately fits the set of 256 SEM images of sludge.

The self-similarity of objects identified on the surface of SEM images of sludge is indicative of their fractal nature and structure. The accumulated data support the determination of surface fractal dimension D_a [27] for every group of analyzed objects, i.e. for each of 32 types of sludge. Slope s determined for every $lg\ A \sim lg\ P$ plot and raised to the power of 1.5 was adopted as an arbitrary extrapolation of surface fractal dimension D_a to volumetric fractal dimension D_v. It was assumed that flat jagged edges and uneven sludge surfaces can be "extrapolated into space".

It was also assumed that D_v is a "measure" of fractal dimension D of aggregates forming the surface structure of the analyzed sludge. In this sense, the value of D_v is not suitable for direct calculations, but it can be used to a limited extent in comparisons of the analyzed object groups, i.e. Al sludges and Fe sludges.

When the two largest and the two smallest values of s were rejected, the value of D_v as a mean of four replications (with standard deviation SD) was calculated for every type of sludge. The database of D_v values was ultimately reduced from 256 to 128 items for 32 types of sludge in four replications each.

Table 3.

The values of 32 average fractal dimensions D_v with standard deviation SD and 32 average values of coefficient of determination R^2 are presented in Table 3. Even a cursory evaluation of data shown in Table 3 indicates that all D_v values of Al sludges are higher than the D_v values of Fe sludges. The above is validated by previous observations of direct SEM images (Fig. 4 and 5) of both sludge groups. The condensed structure of Al sludges (higher D_v) and the jagged and porous structure of Fe sludges (lower D_v) were thus mathematically validated. D_v values of Al sludges ranged from 1.3713 to 1.4858, and D_v values of Fe sludges – from 1.2478 to 1.3564. The average value of D_v was determined at 1.423±0.027 for Al sludges and 1.294±0.032 for Fe sludges. The results of a quantitative comparison of spherical $\{Al(OH)_3\}$ and rod/wire-shaped $\{Fe(OH)_3\}$ aggregate units had been anticipated in view of the described differences in the shape of the compared colloidal particles. The vague differences in the

structure of images shown in Figures 4 and 5 (excluding DSes-Fe with Synten Orange P-4RL) were thus quantitatively described and documented.

The coagulation-flocculation of DDS effluents was the most complex process in the group of four analyzed treatment methods. The resulting aggregates contain colloidal particles of Al or Fe hydroxide and a) organic substances and other compounds found in milk powder, b) colloidal particles $(SiO_2)_n$, P-PO_4, dyes and pH adjusting agents. Electrocoagulated DSre effluents constitute the simplest system for theoretical discussions and modeling because they contain only colloidal particles of Al or Fe hydroxide, P-PO_4 and dyes. HCl, used as a pH adjusting agent, contributes to a minor increase in the ionic strength of the solution which is determined by NaCl in every type of wastewater. The unit for modeling aggregation-flocculation is presented schematically in Figure 7.

Fig. 7.

At pH < 6, colloidal particles of Al and Fe hydroxides and also hydrolysis species are positively charged [4]. The above sols are stable due to electrostatic repulsion between particles, and they can act as colloidal adsorbents. The surface of adsorbent particles features negatively charged phosphate ions which, in turn, are covered with dye particles. Dye particles on the surface of colloidal Al and Fe hydroxides cannot be adsorbed. It was experimentally demonstrated that the addition of an aqueous solution of Al^{3+} or Fe^{3+} ions to an aqueous dye solution does not destabilize the system. Coagulation and electrocoagulation do not take place, flocs are not formed in the system, and red pigmentation of the solution persists. The system is destabilized by coagulation or electrocoagulation, and dyes are completely removed from effluents only in the presence of phosphates. In Figure 7, dye particles are bonded to the surface of $\{Al(OH)_3\}$ or $\{Fe(OH)_3\}$ colloidal particles by P-PO_4.

Phosphate adsorption on the surface of a colloidal adsorbent significantly weakens electrostatic repulsion which stabilized the colloidal solution. By destabilizing the colloidal system, P-PO_4 facilitates the initiation of aggregation, and a collision between two new particles and adsorbed phosphates produces a dimer. Theoretically, a dimer and a particle can form a trimer. Yet in view of the available research findings [32] and our observations, collisions where two dimers produce a tetramer, two tetramers produce an octamer or, possibly, a tetramer with an octamer, are more probable. This aggregation process leads to the complete destabilization of a colloidal system and the formation of aggregates-flocs which fall to the bottom of the vessel and become separated from the treated effluent phase. Falling

flocs effectively bind/capture dye particles in the process of sweep flocculation, separating them from the liquid phase of treated wastewater. The described process leads to the complete removal of dyes from treated effluents. The quantity (weight) of pigment particles removed during sweep flocculation is similar to that observed during phosphate sorption on a colloidal adsorbent. In most cases, > 90% of P-PO_4, and > 90% of the pigment are separated from the liquid phase of treated wastewater.

Fig. 8.

Two extreme structures of a model wastewater floc, described by fractal dimensions 1.4727 for DSre-Al and 1.2655 for DSre-Fe, are presented schematically in Figure 8. DSre effluents were selected because electrocoagulation in a recirculation system has a variety of practical applications, and the quality and structure of sludge is an important technological parameter. Distribution charts in Figure 6 indicate that aggregates with diameter of up to 150 μm were the predominant "fraction" in >80% of the studied objects. Within the above range, the average size of a DSre-Al aggregate-floc was determined at 58.5 μm (18-150 μm), which was equal to its diameter, and the average size of a DSre-Fe aggregate-floc – at 69.5 μm (30-150 μm). The structure of DSre-Al and DSre-Fe sludge objects was simulated with model $\{Al(OH)_3\}$ colloidal particles with average diameter of R = 165 nm proposed by Macedo [33] and cylindrical $\{Fe(OH)_3\}$ particles. Due to an absence of uniform data regarding the size of $\{Fe(OH)_3\}$ cylinders [30-31], the length of a colloidal $\{Fe(OH)_3\}$ particle equal to the diameter of a spherical $\{Al(OH)_3\}$ particle, i.e. 165 nm, was used in calculations. The data were used to model statistical DSre-Al and DSre-Fe aggregate-flocs. The number of units per floc was calculated:

a) DSre-Al aggregate-floc $\left(\frac{58.5 \cdot 1000\ nm}{165\ nm}\right)^{1.4727} = 5685$ $\{Al(OH)_3\}$ units,

b) DSre-Fe aggregate-floc $\left(\frac{69.5 \cdot 1000\ nm}{165\ nm}\right)^{1.2655} = 2095$ $\{Fe(OH)_3\}$ units.

A comparison of DSre-Al and DSre-Fe aggregates-flocs indicates that every volumetric unit contains 2.7-fold more spherical $\{Al(OH)_3\}$ units than $\{Fe(OH)_3\}$ cylindrical and rod-shaped units. The differences between the examined objects were quantified. The respective number of units in the analyzed aggregates was extrapolated to the projection of a given aggregate-floc onto a plane:

a) DSre-Al aggregates-flocs $(5685)^{0.66} = 318$ {$Al(OH)_3$},

b) DSre-Fe aggregates-flocs $(2095)^{0.66} = 163$ {$Fe(OH)_3$}.

A total of 318 spherical {$Al(OH)_3$} units and 163 cylindrical {$Fe(OH)_3$} units obtained by cluster-cluster aggregation were arranged in a circle with the same diameter (simulated volumetric unit). The diagrams of CA-formed flocs are similar to the models obtained by DLCA [25].{$Al(OH)_3$} flocs have a more compact structure (Fig. 8a), whereas {$Fe(OH)_3$} flocs are characterized by jagged edges (Fig. 8b).

The quality and structure of various sludges can be compared quantitatively based on the determined values of fractal dimension D_v of aggregates in a given sludge. The variations in the value of D_v are determined by at least three principal sludge parameters: a) sorption capacity during sweep flocculation [1, 4], b) susceptibility to sedimentation or floating separation from the treated wastewater phase [22], and c) susceptibility to dehydration in an ultracentrifuge or a filter press. Sludge flocs with well-developed and jagged surface structure, i.e. flocs characterized by a lower value of D_v, have a greater ability to absorb pollutants during sweep flocculation than flocs characterized by a more compact structure, higher value of D_v and smaller specific surface area. In this respect, aggregates with a low value of D_v should increase the effectiveness of wastewater treatment during sweep flocculation. Sludges formed by aggregates with a lower value of D_v should be easier to separate from the phase of effluents treated by floatation than sedimentation. The sedimentation of such aggregates-flocs is slower, and the resulting sludge is characterized by high volume. In theory, sludges with lower D_v should be less susceptible to dehydration than sludges with higher D_v, which could be less technologically efficient. It could seem that dense sludge aggregates which have a higher value of D_v and contain less water should be more susceptible to dehydration or "self-dehydration" [15]. This observation is debatable because Waite [22] argued that SO_4^{2-} ions present in PIX are responsible for "structural" decomposition of sludge flocs and that "looser" aggregates support filtration (sludge separation) and dehydration of filtered sludge. The above considerations lead to a dilemma of choice between sludges with lower D_v which more effectively absorb pollutants during sweep flocculation and sludges with higher D_v which are more susceptible (or not) to separation and dehydration. Further research is needed to work out a compromise.

In the introduction, two principal types of aggregation were identified: particle-cluster aggregation (PA) and cluster-cluster aggregation (CA). The involvement of indirect

mechanisms was stipulated, e.g. PA in the initial stages of aggregation and CA in the final stages of the process. It has been widely documented [34] that aggregates formed during PA are characterized by higher fractal dimension D than aggregates produced during CA. The results of sludge analyses described in this study do not support unambiguous determination of processes responsible for the formation of sludge aggregates which have been described by SEM and Image Analysis. Al aggregates are characterized by higher fractal dimensions D_v than Fe aggregates. Numeric values of D_v were obtained by data conversion, therefore, they are only a measure of fractal dimension D, and they can only be used in comparisons of structures analyzed by the same method.

Earlier research has showed [35] that pre-polymerized coagulants favour the "adsorption-charge neutralization" mechanism. The Al-coagulant used in this research (PAC) is a pre-polymerized coagulant, while the Fe-coagulant (PIX) is ferric sulphate with no polymerization. Thus it can be expected that Fe-coagulant was predominantly forming CA type aggregates due to hydroxide-hydroxide aggregation, while Al-coagulants might form also PA type aggregates, where particles aggregate with hydroxides. In view of the above and based on experimental data, it can be assumed that PA could be involved more into Al aggregates-flocs formation than into Fe aggregates-flocs.

The principles of coagulation, aggregation and flocculation and fractal dimensions of sludge aggregates formed by coagulation-flocculation [24] point to diffusion-limited cluster-cluster aggregation (DCLA) whose rate is determined by cluster diffusion. Reaction-limited cluster-cluster aggregation (RLCA) can be ruled out due to low values of D and low concentrations of potential reagents.

4. Conclusions

The applied image analysis method revealed that the examined wastewater sludges were composed of self-similar aggregates-flocs with fractal properties. $lgA \sim lgP$ plots (A - area, P - perimeter) support the determination of surface fractal dimension D_a which is statistically justified by the high value of the coefficient of determination R^2. SEM images and the value of volumetric fractal dimension D_v (extrapolated from D_a) quantitatively describe sludge aggregates-flocs. Al sludge aggregates were characterized by higher values of D_a and D_v than Fe sludge flocs. The higher density of Al sludges and jagged structure of Fe sludges, which were observed in SEM analyses, were thus quantitatively validated. Our experiment revealed that phosphate ions are required for the destabilization of colloid-dye systems. A model for P-PO_4 and dye sorption on a colloidal sorbent comprising $Al(OH)_3\}$ or $\{Fe(OH)_3\}$

was proposed. The results also indicate the particle-cluster type aggregation could be involved into Al aggregates-flocs forming, while cluster-cluster type aggregation was predominating in Fe agggreagtes-flocs formation. The technological consequences of the impact exerted by D_v on sweep flocculation, effluent separation and dehydration were determined based on a graphic simulation of aggregates-flocs made of $\{Al(OH)_3\}$ and $\{Fe(OH)_3\}$ particles. The modeled processes of P-PO_4 sorption and dye sweep flocculation as well as the simulated images of aggregates-flocs confirmed that DLCA was the process responsible for the formation of the examined sludge.

Acknowledgement

The authors acknowledge the contribution from the research collaboration through the IMPREC project which is funded by the Polish-Norwegian Research Fund and also supported by the European Union within the European Social Fund

KAPITAŁ LUDZKI
NARODOWA STRATEGIA SPÓJNOŚCI

UNIA EUROPEJSKA
EUROPEJSKI
FUNDUSZ SPOŁECZNY

References

[1] W.Yu, T. Liu, J. Gregory , G. Li, H. Liu, J. Qua, Aggregation of nano-sized alum–humic primary particles, Sep. Purif. Technol. 99 (2012) 44 - 49.

[2] A. Stradner, H. Sedgwick, F. Cardinaux, W.C.K. Poon, S.U. Egelhaaf, P. Schurtenberger, Equilibrium cluster formation in concentrated protein solutions and colloids, Nature. 432 (2004) 492 - 495.

[3] G. Yang, P. Biswas, Computer Simulation of the Aggregation and Sintering Restructuring of Fractal-like Clusters Containing Limited Numbers of Primary Particles, J. Colloid Interface Sci. 211 (1999) 142 - 150.

[4] J. Duan, J. Gregory, Coagulation by hydrolyzing metal salts, Adv. Colloid Interface Sci. 100 - 102 (2003) 475 - 502.

[5] L. Smoczynski, P. Mroz, R. Wardzynska, B. Załeska-Chrost, K. Dłuzynska, Computer Simulation of Flocculation of Suspended Solids, Chem. Eng. J. 152 (2009) 146 - 150.

[6] N. Kallay, S. Žalac, Introduction of the Surface Complexation Model into the Theory of Colloid Stability, Croat. Chem. Acta. 74 (3) (2001) 479 - 497.

[7] S. Zodi, O. Potier, F. Lapicque, J.P Leclerc, Treatment of the textile wastewaters by electrocoagulation: Effect of operating parameters on the sludge settling characteristics, Sep. Purif. Technol. 69 (2009) 29 - 36.

[8] D. Cordell, J.O. Drangert, S. White, The story of phosphorus: Global food security and food for thought, Global Environ. Chang. 19 p. (2009) 292 - 305.

[9] J.M. Prats-Montalban, A. Ferrer, R. Bro, T. Hancewicz, Prediction of skin quality properties by different Multivariate Image Analysis methodologies, Chemometr. Intell. Lab. 96 (2009) 6 - 13.

[10] L. Smoczynski, R. Wardzynska, B. Pierozynski, Computer Simulation of Polydispersive Sol Coagulation Process, Can. J. Chem. Eng. 91 (2013) 302 - 310.

[11] L. Smoczynski, Z. Bukowski, R. Wardzynska, B. Załeska-Chrost, K. Dłuzynska, Simulation of coagulation, flocculation and sedimentation, Water Environ. Res. 81 (4) (2009) 48 – 356 (9).

[12] E. Butler, Y-T. Hung, R. Yu-Li Yeh, M.S. Al Ahmad, Electrocoagulation in Wastewater Treatment, Water 3 (2011) 495 - 525.

[13] S. Irdemez, N. Demircioglu, Y.S. Yıldız, Z. Bingul, The effects of current density and phosphate concentration on phosphate removal from wastewater by electrocoagulation using aluminum and iron plate electrodes, Sep. Purif. Technol. 52 (2006) 218 - 223.

[14] M.S. Secula, I. Cretescu, S. Petrescu, An experimental study of indigo carmine removal from aqueous solution by electrocoagulation, Desalination 277 (2011) 227 - 235.

[15] L. Smoczynski, Aggregation of the Silica Suspension by Al-Coagulants, Pol. J. Chem. 74 (2000) 1617 - 1624.

[16] R. Jullien, P. Meakin, Simple models for the restructuring of 3-dimensional ballistic aggregates, J. Colloid Interface Sci. 127 (1989) 265 - 272.

[17] B.B. Mandelbrot, The Fractal Geometry of Nature, Freeman, San Francisco, 1982.

[18] F.G. Meng, H.M. Zhang, Y.S. Li, X.W. Zhang, F.L. Yang, J.N. Xiao, Cake layer morphology in microfiltration of activated sludge wastewater based on fractal analysis, Sep. Purif. Technol. 44 (2005) 250 - 257.

[19] Y.Q. Zhao, Settling behaviour of polymer flocculated water-treatment sludge II: effects of floc structure and floc packing, Sep. Purif. Technol. 35 (2004) 175 - 183.

[20] P. Meakin, The Effects of Reorganization Processes on Two-Dimensional Cluster-Cluster Aggregation. J. Colloid Interface Sci. 112 (1986) 187 - 194.

[21] R. Pastor-Satorras, J.M. Rubí, Particle-cluster aggregation with dipolar interactions, Phys. Rev. E 51 (6) (1995) 5994 - 6003.

[22] T.D. Waite, Measurement and implications of floc structure in water and wastewater treatment, Colloids Surface A 151 (1999) 27 - 41.

[23] Z. Yang, H. Yang, Z. Jiang, X. Huang, H. Li, A. Li, R. Cheng, A new method for calculation of flocculation kinetics combining Smoluchowski model with fractal theory, Colloids Surface A 423 (2013) 11 - 19.

[24] L. Smoczynski, R. Wardzynska, Study on Macroscopic Aggregation of Silica Suspension and Sewage, J. Colloid Interface Sci. 183 (1996) 309 - 314.

[25] D. Asnaghi, M. Carpineti, M. Giglio, M. Sozzi, Coagulation kinetics and aggregate morphology in the intermediate regimes between diffusion-limited and reaction-limited cluster aggregation, Phys. Rev. A 45 (2) (1992) 1018 - 1022.

[26] S.C. Jr Ferreira, S.G. Alves, A.F. Brito, J.G. Moreira, Morphological transition between diffusion-limited and ballistic aggregation growth patterns, Phys. Rev. E 71 (5) (2005).

[27] J. Dziuba, A. Babuchowski, M. Smoczynski, Z. Smietana, Fractal analysis of caseinate structure, Int. Dairy J. 9 (1999) 287 - 292.

[28] L. Smoczynski, K. Munska, B. Pierozynski, Electrocoagulation of synthetic wastewater, Water Sci. Technol. 67(2) (2013) 404 - 409.

[29] S. Verma, B. Prased, I.M. Mishra, Pretreatment of petrochemical wastewater by coagulation and the sludge characteristics. J. Hazard. Mater. 178 (2010) 1055 - 1064.

[30] W. Haas, M. Zrinyi, H.G. Kilian, B. Heise, Structural analysis of anisometric colloidal iron(III)-hydroxide particles and particle-aggregates incorporated in poly(vinyl-acetate) networks, Colloid Polym. Sci. 271 (1993) 1024 - 1034.

[31] S. Rohrsetzer, I. Paszli, F. Csempesz, S. Ban, Colloidal stability of electrostatically stabilized sol particles. Part I: The role of hydration in coagulation and repeptization of ferric hydroxide sol, Colloid Polym. Sci. 270 (1992) 1243 - 1251.

[32] di Stasio, Stefano, Konstandopoulos, G. Athanasios, Kostoglou, Margaritis, Cluster-cluster Aggregation Kinetics and Primary Particle Growth of Soot Nanoparticles in Flame by Light Scattering and Numerical Simulations, J. Colloid Interface Sci. 247 (2002) 33 - 46.

[33] M.I.F. Macedo, C.C. Osawa, C.A. Bertran , Sol-Gel Synthesis of Transparent Alumina Gel and Pure Gamma Alumina by Urea Hydrolysis of Aluminum Nitrate, J. Sol-Gel Sci. Techn. 30 (2004) 135 - 140.

[34] M. Matsushita, Experiments on Aggregations, Research of Pattern Formation, edited by R. Takaki, pp. 169 -175.

[35] H. Ratnaweera, J. Fettig, H. Ødegaard, Particle and phosphate removal mechanisms with prepolymerized aluminum coagulants. In: Chemical water and wastewater treatment II, Hahn, H.H. and Klute, R. (Eds.), Springer-Verlag, Berlin, 1992, pp. 3-17.

Tab. 1.

dyestuff / waste-water		red synt. P-3BL	red direct 6B	red gryf. G	orange synt. P-4RL
DDS	PAC	139±0.8%	139±0.8%	139±0.8%	139±0.8%
	pH	5.0	5.0	5.0	5.0
	PIX	171±0.4%	171±0.4%	171±0.4%	171±0.4%
	pH	5.0	5.0	5.0	5.0
DSch	PAC	139±0.8%	139±0.8%	139±0.8%	139±0.8%
	pH	4.5	4.0	3.5	4.0
	PIX	171±0.4%	171±0.4%	171±0.4%	171±0.4%
	pH	4.0	4.0	3.5	4.0
DSes	Al	601±2.5%	613±2.8%	614±3.4%	618±3.4%
	pH	4.5	4.0	3.5	4.0
	Fe	225±2.2%	221±2.7%	554±1.6%	234±3.4%
	pH	4.0	4.0	3.5	4.0
DSre	Al	107.14	107.14	107.14	107.14
	pH	6.0	6.0	6.0	6.0
	Fe	332.93	332.93	332.93	332.93
	pH	4.0	4.0	4.0	4.0

Tab. 2.

waste-water	dyestuff	red synt. P-3BL	red direct 6B	red gryf. G	orange synt. P-4RL
DDS	PAC: P-PO_4	95 ± 3.6	95 ± 8.9	96 ± 4.8	94.5 ± 13.3
	dyestuff	94 ± 11	97 ± 4.5	96±15.1	90±6.9
	PIX: P-PO_4	97.5±2.7	96±6.8	98±12.6	97±14.7
	dyestuff	96±16.5	98±17.7	97±8.6	91±6.2
DSch	PAC: P-PO_4	38±7.7	41±8.8	37±4.2	39±4.5
	dyestuff	99±16.7	99±9.9	86±14.4	98±11.1
	PIX: P-PO_4	95±15.5	85±7.7	56±11.3	92±17.8
	dyestuff	97.5±14.5	91±10	20±11.2	92.5±10.9
DSes	Al: P-PO_4	88±4.4	73±9.4	38±1.5	90±11.6
	dyestuff	97±14.6	67±12.1	14.0±2.3	94±18.2
	Fe: P-PO_4	95±18.2	90±7.3	70±3.0	93±6.8
	dyestuff	95.5±17.7	89±4.0	76±5.0	92±9.8
DSre	Al: P-PO_4	91±5.2	98±10.5	65±1.4	95±20.3
	dyestuff	98±15.4	99±3.5	21±9.9	97.5±9.1
	Fe: P-PO_4	89±7.5	81±16.6	66±4.7	93±19.7
	dyestuff	79±4.5	76±13.7	25±13.5	88±14.8

Tab. 3.

dyestuff / waste-water		red synt. P-3BL		red direct 6B		red gryf. G		orange synt. P-4RL	
		D_v $\pm SD_D$	R^2 $\pm SD_R$	D_v $\pm SD_D$	R^2 $\pm SD_R$	D_v $\pm SD_D$	R^2 $\pm SD_R$	D_v $\pm SD_D$	R^2 $\pm SD_R$
DDS	PAC	1.4196 ±0.0216	0.9624 ±0.0147	1.4322 ±0.0396	0.9765 ±0.0118	1.4066 ±0.0067	0.95895 ±0.0112	1.4383 ±0.0248	0.9509 ±0.0195
	PIX	1.2478 ±0.0105	0.9653 ±0.0066	1.2814 ±0.0058	0.93705 ±0.0196	1.2832 ±0.0121	0.9431 ±0.0106	1.2784 ±0.0116	0.9507 0.0071
DSch	PAC	1.4394 ±0.0579	0.9757 ±0.0072	1.4417 ±0.0109	0.968 ±0.0200	1.3713 ±0.0063	0.9747 ±0.0061	1.3996 ±0.0172	0.9713 ±0.0074
	PIX	1.2588 ±0.0102	0.9584 ±0.0119	1.2843 ±0.0139	0.9591 ±0.0121	1.2868 ±0.0276	0.9673 ±0.0155	1.2811 ±0.0373	0.9707 ±0.0035
DSes	Al	1.4127 ±0.0352	0.9667 ±0.0106	1.3867 ±0.0124	0.9751 ±0.0086	1.4125 ±0.0211	0.9612 ±0.0048	1.4201 ±0.0257	0.9697 ±0.0085
	Fe	1.2783 ±0.0273	0.9618 ±0.0103	1.3412 ±0.0051	0.9741 ±0.0079	1.2635 ±0.0349	0.9474 ±0.0203	1.2920 ±0.0096	0.9632 ±0.0065
DSre	Al	1.4402 ±0.0268	0.9617 ±0.0138	1.4243 ±0.0256	0.9656 ±0.0034	1.4858 ±0.0052	0.9743 ±0.0086	1.4449 ±0.0208	0.9674 ±0.0165
	Fe	1.2876 ±0.0180	0.9570 ±0.0121	1.3416 ±0.0062	0.9429 ±0.0123	1.3275 ±0.0166	0.9616 ±0.0071	1.3564 ±0.0304	0.9568 ±0.0155

Graphical Abstract (for review)

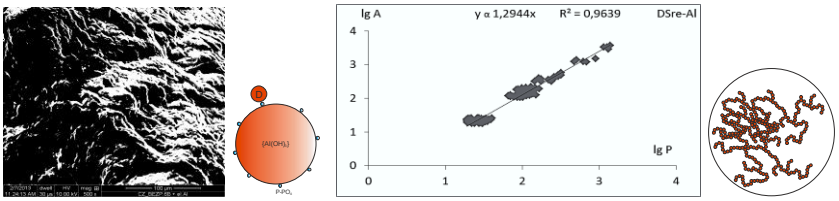

image → particle log(*Area*) α log(*Perimeter*) → fractal dimension of flock

Highlights

Scanning electron microscopy (SEM) images of sludge obtained by chemical treatment and electrocoagulation of wastewater are presented. *log(Area)~ log(Perimeter)* plots of self-similar objects give the fractal dimension *D*. Al-aggregates made of spherical units are always characterized by a higher value of *D* than Fe-aggregates comprising cylindrical units. Flocculation of the sol-dye system was not observed, and it constitutes the basis for modeling the removal of P-PO_4 and dyes from treated wastewater.

Figures

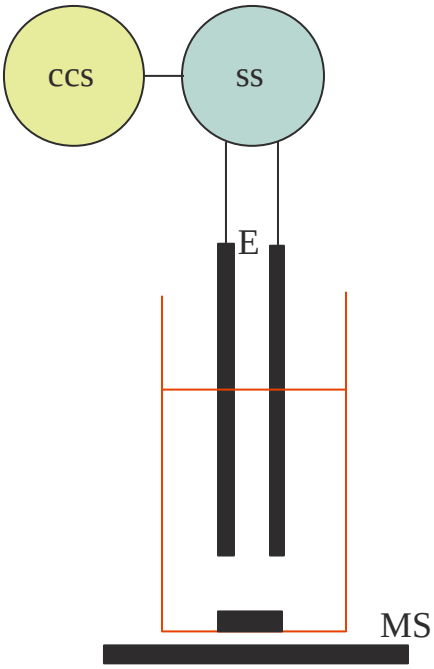

Figures

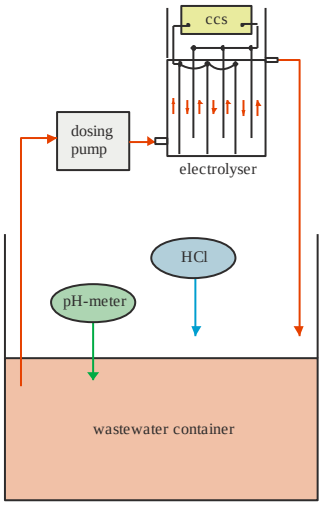

Figures

Al a) b) c) d)

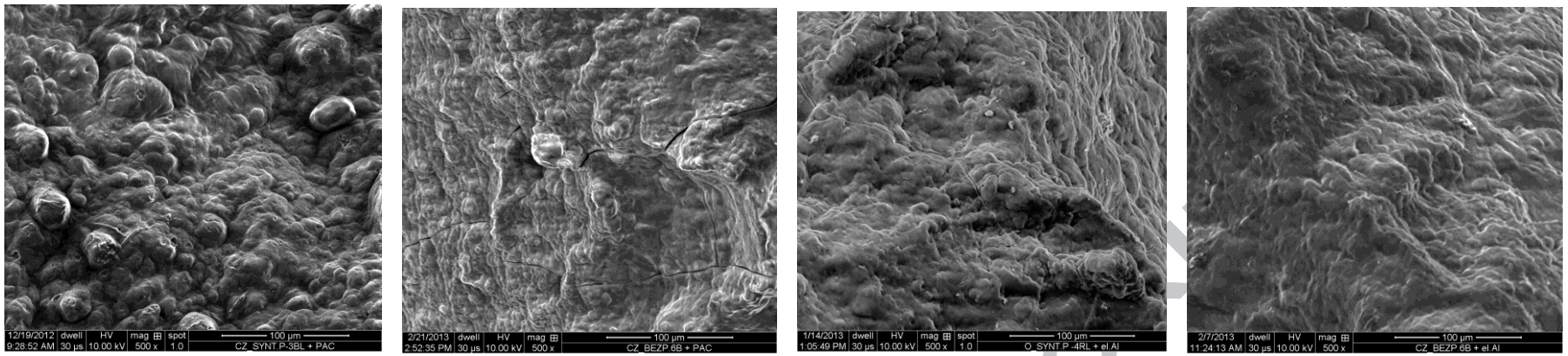

Fe

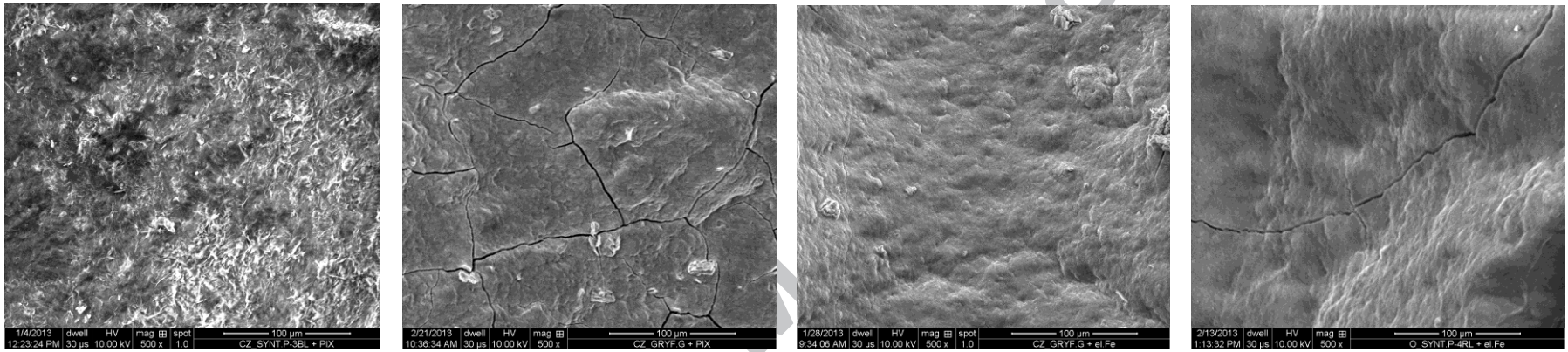

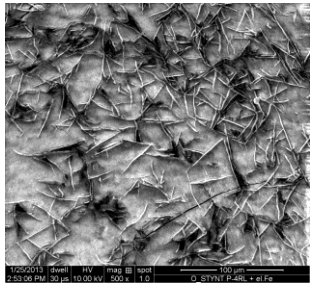

Figures

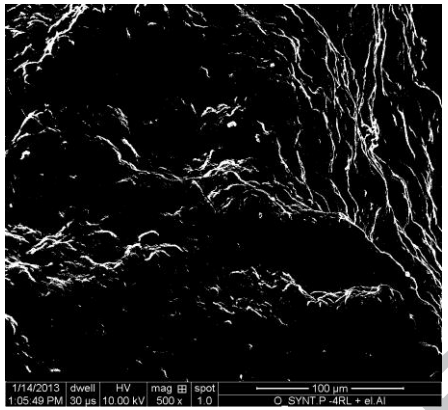

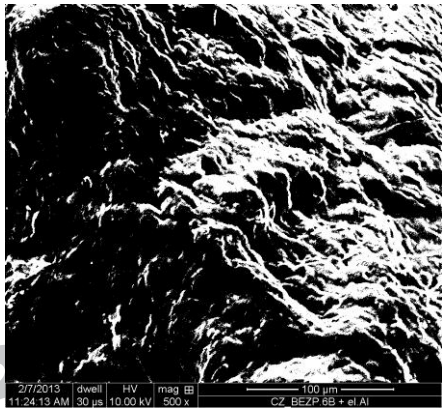

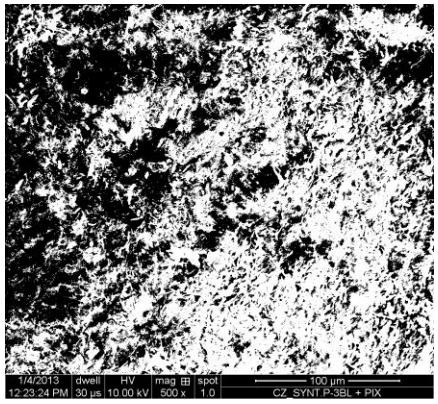

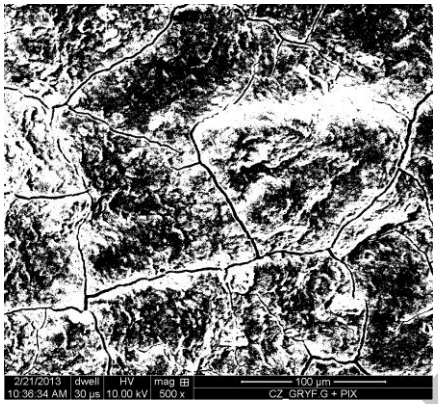

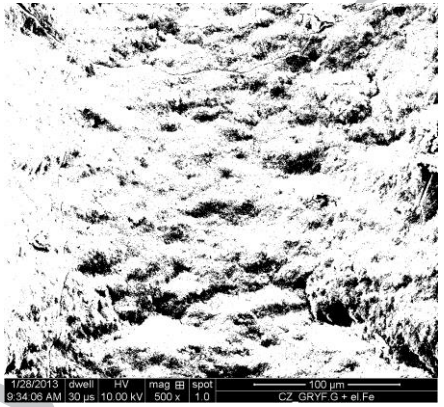

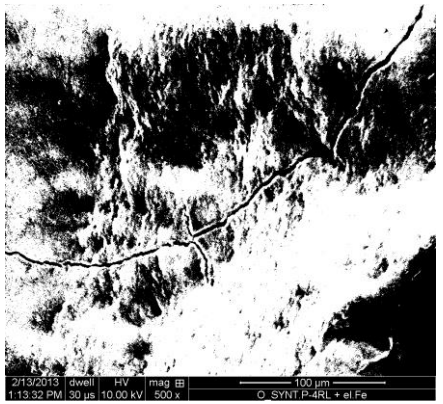

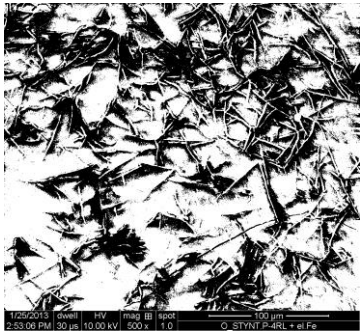

Figures

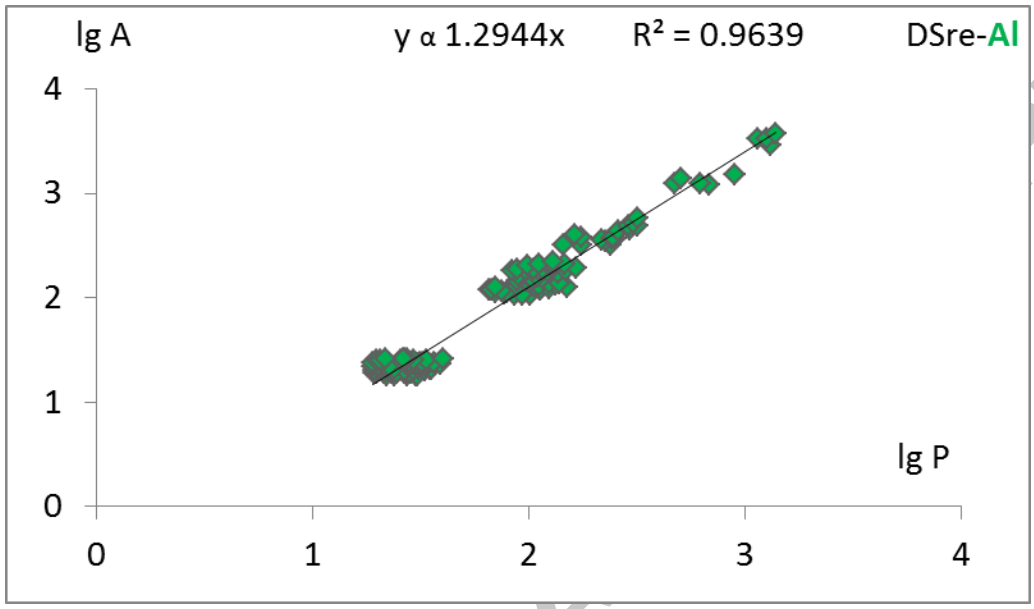

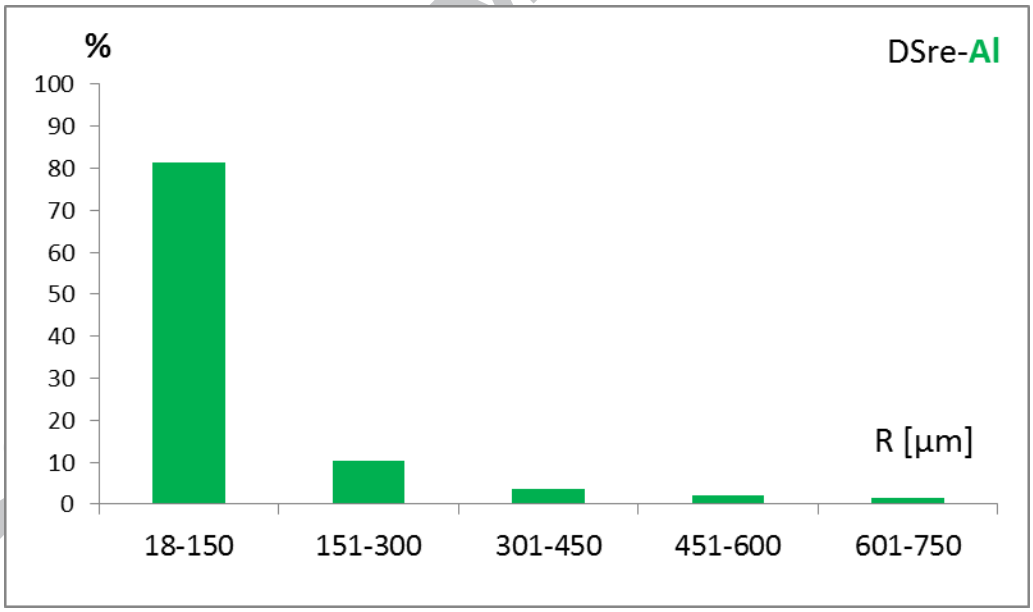

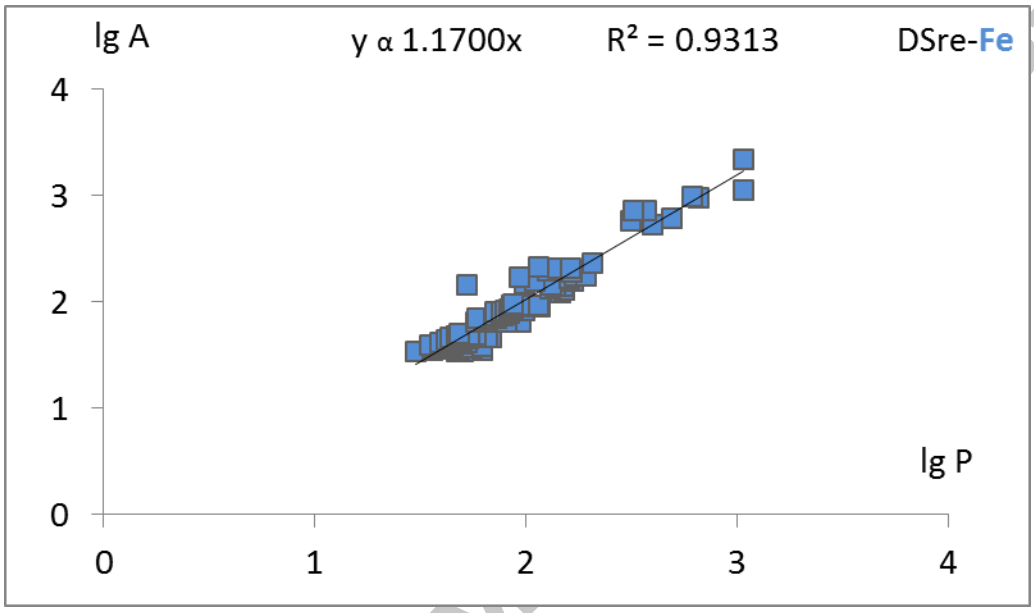

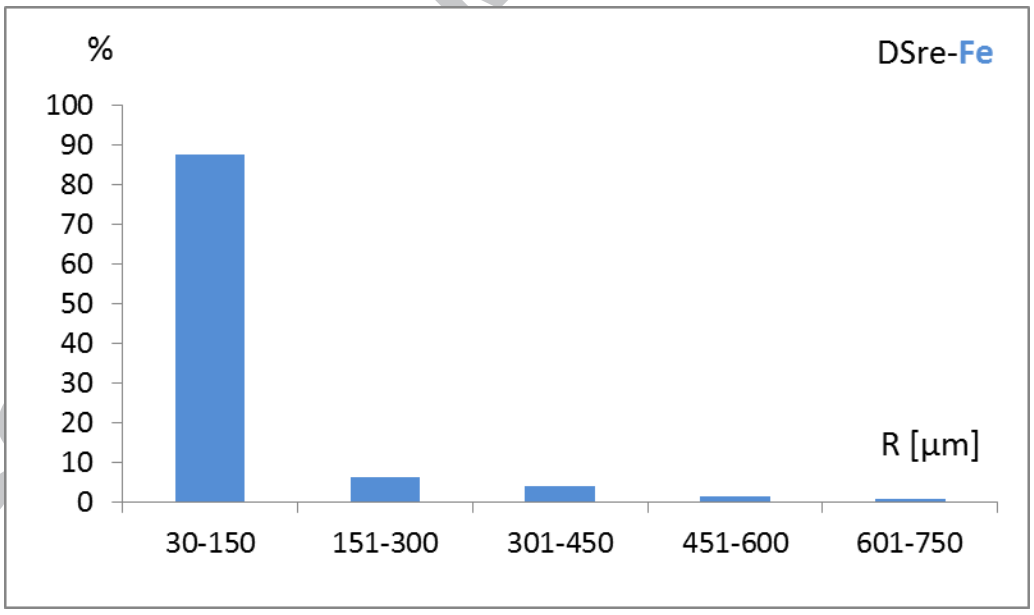

Figures

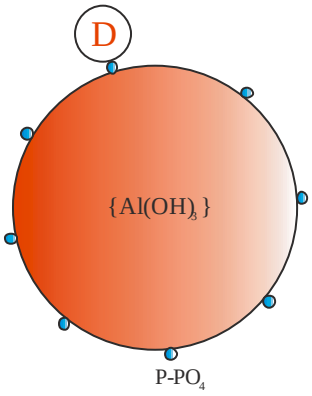

a)

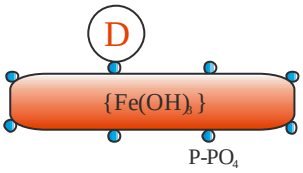

b)

Figures

a)

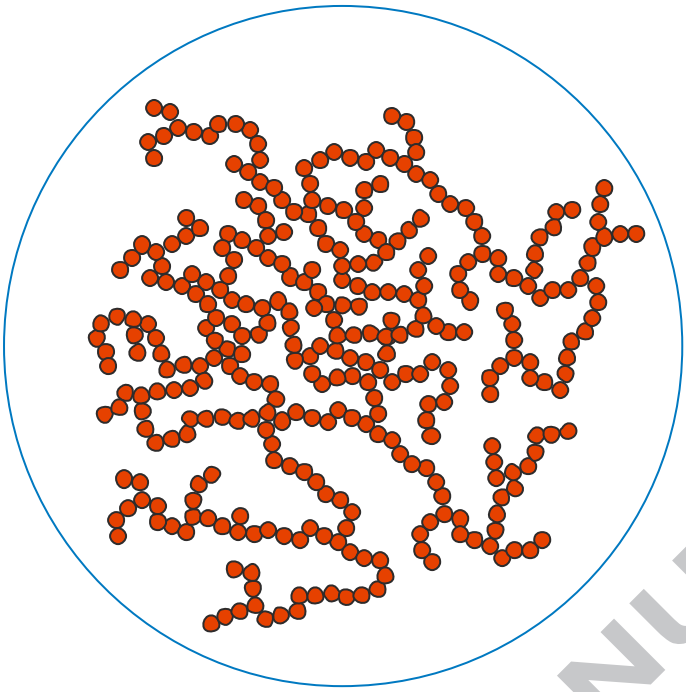

b)

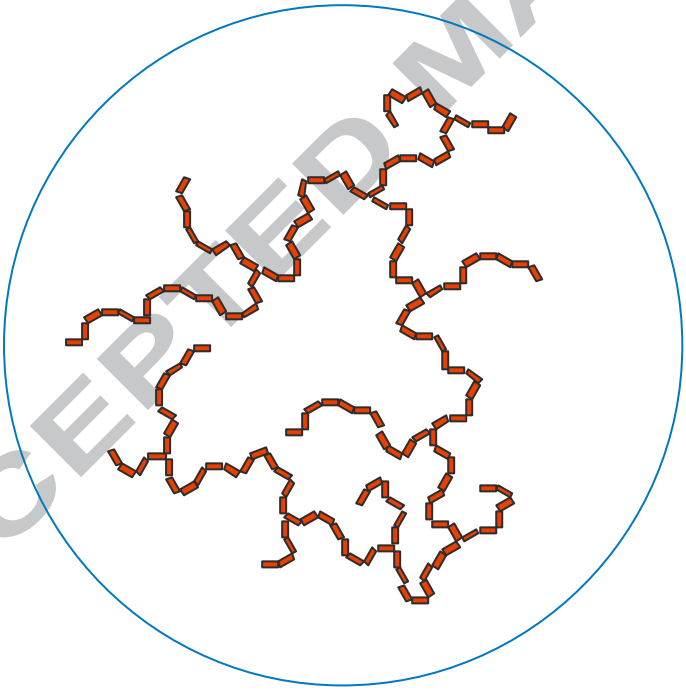

a)

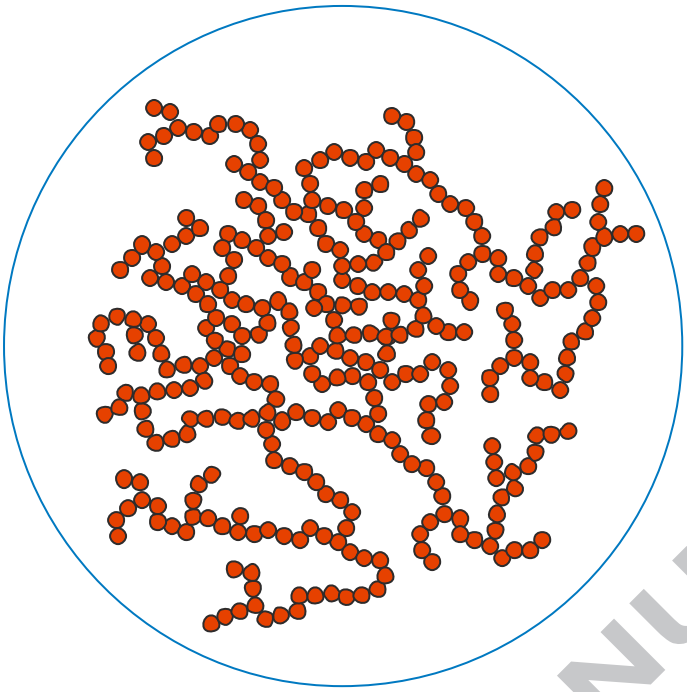

b)